

*EMM/DO/...*

**Final Report**

**submitted to**

**NATIONAL AERONAUTICS AND SPACE ADMINISTRATION  
GEORGE C. MARSHALL SPACE FLIGHT CENTER, ALABAMA 35812**

**May 25, 1994**

**for Contract NAS8 - 38609**

**Delivery Order 83**

**entitled**

**Study on Contaminants on Flight and  
Other Critical Surfaces**

**by**

**Gary L. Workman Ph.D.  
Principal Investigator**

**Charles Hughes and  
William F. Arendale, Ph.D.**

**In-line Process Control Laboratory  
Center for Automation & Robotics  
University of Alabama in Huntsville  
Huntsville, Alabama 35899**

**N94-35447**

**Unclas**

**G3/25 0013759**

**(NASA-CR-193975) STUDY ON  
CONTAMINANTS ON FLIGHT AND OTHER  
CRITICAL SURFACES Final Report  
(Alabama Univ.) 35 p**



# Report Documentation Page

1. Report No.		2. Government Accession No.		3. Recipient's Catalog No.	
4. Title and Subtitle <b>Study on Contaminants on Flight and Other Critical Hardware Production</b>			5. Report Date		
			6. Performing Organization Code <b>UAH/CAR</b>		
7. Author(s) <b>Gary L. Workman</b>			8. Performing Organization Report No.		
			10. Work Unit No.		
9. Performing Organization Name and Address <b>University of Alabama in Huntsville Research Institute Box 212 Huntsville, AL 35899</b>			11. Contract or Grant No. <b>NAS8-38609 D.O. 83</b>		
			13. Type of Report and Period Covered <i>Final Quarterly</i>		
12. Sponsoring Agency Name and Address			14. Sponsoring Agency Code <b>NASA/MSFC</b>		
			15. Supplementary Notes		
16. Abstract					
<p>The control of surface contamination in the manufacture of space hardware can become a critical step in the production process. Bonded surfaces have been shown to be affected markedly by contamination. It is important to insure surface cleanliness by preventing contamination prior to bonding. In this vein techniques are needed in which the contamination which may affect bonding are easily found and removed. Likewise, if materials which are detrimental to bonding are not easily removed, then they should not be used in the manufacturing process.</p> <p>This study will address the development of techniques to locate and quantify contamination levels of particular contaminants. With other data becoming available from MSFC and its contractors, this study will also quantify how certain contaminants affect bondlines and how easily they are removed in manufacturing.</p>					
17. Key Words (Suggested by Author(s)) <b>Contamination, Bonding Surface Inspection Spectroscopy, Chemometrics</b>			18. Distribution Statement		
19. Security Classif. (of this report)		20. Security Classif. (of this page)		21. No. of pages	22. Price

**Final Report**

**submitted to**

**NATIONAL AERONAUTICS AND SPACE ADMINISTRATION  
GEORGE C. MARSHALL SPACE FLIGHT CENTER, ALABAMA 35812**

**May 25, 1994**

**for Contract NAS8 - 38609**

**Delivery Order 83**

**entitled**

**Study on Contaminants on Flight and  
Other Critical Surfaces**

**by**

**Gary L. Workman Ph.D.  
Principal Investigator**

**Charles Hughes and  
William F. Arendale, Ph.D.**

**In-line Process Control Laboratory  
Center for Automation & Robotics  
University of Alabama in Huntsville  
Huntsville, Alabama 35899**

## TABLE OF CONTENTS

1.0 Introduction	1
2.0 Research Objectives	2
3.0 Optical Fiber Spectrometry Concepts	3
4.0 Chemometric Principles	3
5.0 Experimental Approaches	5
6.0 Tape Residue Studies	5
7.0 Integrating Sphere Test	16
8.0 Spectra for 7075 Al Hydroxides Identification	19
9.0 Comparison of NIR Spectrometry and Ellipsometry	27
10.0 Conclusions	31
11.0 Acknowledgements	32
12.0 References	32

## 1.0 Introduction

Maintaining and ensuring clean surfaces for critical applications is an essential requirement in the aerospace industry. Aerospace manufacturing industries are also currently in a state of flux with respect to environmental constraints with the need for solvents and processes which are environmentally benign. For this reason, new and innovative methods of surface characterization are being used to assist in the identification and quantification of contaminants which can cause debonds or degrade bonds in solid rocket motor (SRM) cases. A major advantage to this approach is to avoid preparing bonds with defects. Cost benefits are accrued fairly quickly when one considers the additional costs associated with identification and repair of bond defects versus the minor cost of prevention.

The whole area dealing with the inspection of critical surfaces for undesirable materials provides a useful arena for optical fiber spectrometry, which when coupled with multivariate techniques for chemical analysis, becomes an extremely useful nondestructive testing tool. The type of data which can be obtained from a NIR inspection of surfaces such as SRM's is rather unique in that most other analytical tools are not able to provide such real time information in the manufacturing environment.

Chemometrics is a discipline which uses mathematical and statistical methods for handling, interpreting, and predicting chemical data. Examples of chemometric methods are factor analysis and multivariate analysis. Factor analysis is a multivariate technique for reducing complex data sets to their lowest dimensionality to yield recognizable features and/or predictions. Since there is a strong statistical component in chemometrics, hypothesis testing followed by new postulates and further testing can lead to information that is normally not available by direct observation.

Multivariate calibration is an approach to combining many different instrument channels in order to reduce selectivity problems. The foremost application of multivariate calibration today is in near infra-red spectroscopy (NIR). [1] NIR relies upon multichannel calibrations to provide the selectivity enhancement needed for quantitative spectroscopy in less than perfect conditions. Examples include intact biological samples or turbid process mixtures. General benefits include less sample preparation, higher reliability, and wider range of instrument application.

Optical fiber spectrometry has been demonstrated to be quite versatile in handling unique problems in which spectroscopic analysis can assist in the solution and consequently has become accepted in the food and chemical process industries. With optical fibers as transmissions lines for

spectrometers, spectral information can be obtained in very difficult and sometimes remote locations primarily due to the flexibility of the optical fiber transmission link. Several companies currently market such systems, so that the uniqueness of the concept is expanding into areas once not available for traditional optical spectrometry.

## **2.0 Research Objectives**

The original concepts which were conceived at the beginning of the project were to demonstrate the ability of optical fiber spectrometry to determine contamination levels on solid rocket motor cases in order to identify surface conditions which may not bond properly during production. Adding the capability of the spectral features to identify contaminants with other sensors which might only indicate a potential contamination level provides a real enhancement to current inspection systems such as OSEE. Since the optical fiber probe can easily fit into the same support fixtures as the OSEE, this approach was certainly a reasonable concept to consider.

Earlier work with both NASA/MSFC and Thiokol funding provided the opportunity to explore the capabilities of the optical fiber NIR technique to the following cases:

- HD2 films on D6AC steel and 7075 Aluminum
- Silicone films on D6AC steel and 7075 Aluminum
- Mixtures of HD2 and Silicone films on D6AC steel and 7075 Aluminum
- D6AC steel and 7075 Aluminum plates in controlled temperature and humidity for extended period of time (up to 72 hours).

In each case the results of the investigations were reported in the weekly Surface Contamination Analysis Team meetings and in the appropriate final reports. The primary results of those studies showed that using observations in the NIR spectral region, we were able to:

- Discriminate between HD2 grease and silicone in single or with mixed applications, both qualitatively and quantitatively.
- Detect the various water/hydroxide species that occur on both D6AC and aluminum surfaces under humid conditions.

Since the surface chemistry of D6AC steel is not very well known, very little explanation for the observed spectra could be justified at that time. Although the chemistry of the aluminum hydroxides is reasonably well known; the chemometric analysis of that data provided results that showed differences between the various species, but still the chemistry of the surface reactions and interactions is difficult to explain from these observations alone. Comparisons with frequency doubled fundamental bands reported in references [3-7] confirmed that the equilibrium process going from pseudo-boehmite to bayerite was probably occurring during the experiments.

### **3.0 Optical Fiber Spectrometry Concepts**

Previous reports have given a broad overview of the capabilities and experimental apparatus used for optical fiber spectrometry. During the course of this research we have recorded spectra throughout the range 0.2 to 2.5  $\mu$ , although the results presented here are exclusively from 0.7 to 2.5  $\mu$ .

A significant aspect of the work performed here deals with the reflection/absorption phenomena associated with spectral observation from both D6AC and aluminum 7075 surfaces. The problem that still persists, particularly if an automated procedure is to be developed, lies in the difference observed in spectra depending upon whether the spectral process occurs through reflection (specular or diffuse) or both absorption and reflection. However, progress has been made in the software side, with the use of the Multiple Scattering Correlation (MSC) technique. MCS algorithms are contained in the Unscrambler II software which we have been using to perform PCR and PLS analysis.

### **4.0 Chemometric Principles**

The chemometric concepts used most frequently in this work are basic approaches to improving the signal-to-noise of the acquired spectra and principal component (or factor analysis) to pick out the significant features of the spectra. The procedures performed for the spectra presented here were procedures embedded in commercial software packages. They will be identified during the discussion on the experimental approaches.

For improving the signal-to-noise ratio of the observed spectra, we have made use of polynomial smoothing with both Savitsky-Golay and FFT filters. The routines used in this work are part of the software package SpectrCalc™, marketed by Galaxy Inc. The primary routine uses ESmooth which is a Maximum Likelihood filter that takes an a priori peakshape, such as Gaussian

or Poisson, and then computes the most likely set of peaks which are buried in the spectra. ESmooth is also a maximum entropy filter which allows it to maximize upon the probability states possible.

There are several methods for reducing a data matrix into a smaller number of factors. The algorithm ultimately used depends upon the particular software package or characteristics of the data set being analyzed. The first step is to combine a group of measurements into one data matrix. The measurements may include any set of chemical or physical observations using common instrumental techniques. For example, in the data matrix so formulated, a row may concern a molecular species and a column may concern a particular measurement. Factor analysis will then yield a score matrix that depends on the characteristics of the molecular species and a loading matrix which depends solely on the nature of the matrix.[1] Such a separation provides the analyst with improved insight into the true nature of the phenomena being observed.

The use of MSC for analysis of spectroscopic data arose from two types of applications, turbidity in solutions and reflection measurements. Since the wavelength dependency of light scattering is different from absorbance, one can use data from many different wavelengths to distinguish between light absorption and scattering. The scatter for each sample is estimated relative to that of a reference sample and each sample is corrected so that all samples appear to have the same scatter level as the reference.

The MSC is a general technique for estimating a multiplicative interference when none of the x variables give unique information about this. What is special about MSC is its potential for separating multiplicative scattering variations from the additive chemical information on the basis of the same set of variables.



## 5.0 Experimental Approaches

The major software used to support this work included SpectraCalc and Unscrambler II. Typically spectra were recorded in units of watts and transformed into absorbance using the relationship:

$$A = \log \frac{I}{I_{\text{ref}}}$$

Much work was spent in the beginning of the research in determining what reference surfaces to use for calculating absorbances. The major problem that arises is when a spectral feature goes negative; i.e.  $I < I_{\text{ref}}$  then most of the matrix multiplication techniques are not applicable. Practically, a negative absorbance is undefined, which means that the reference is not valid. Several reference surfaces used in this work include an aluminum or gold mirror, i.e. totally or specular reflecting; barium sulfate i.e., diffuse reflecting, and native surfaces such as D6AC steel or aluminum.

## 6.0 Tape Residue Study

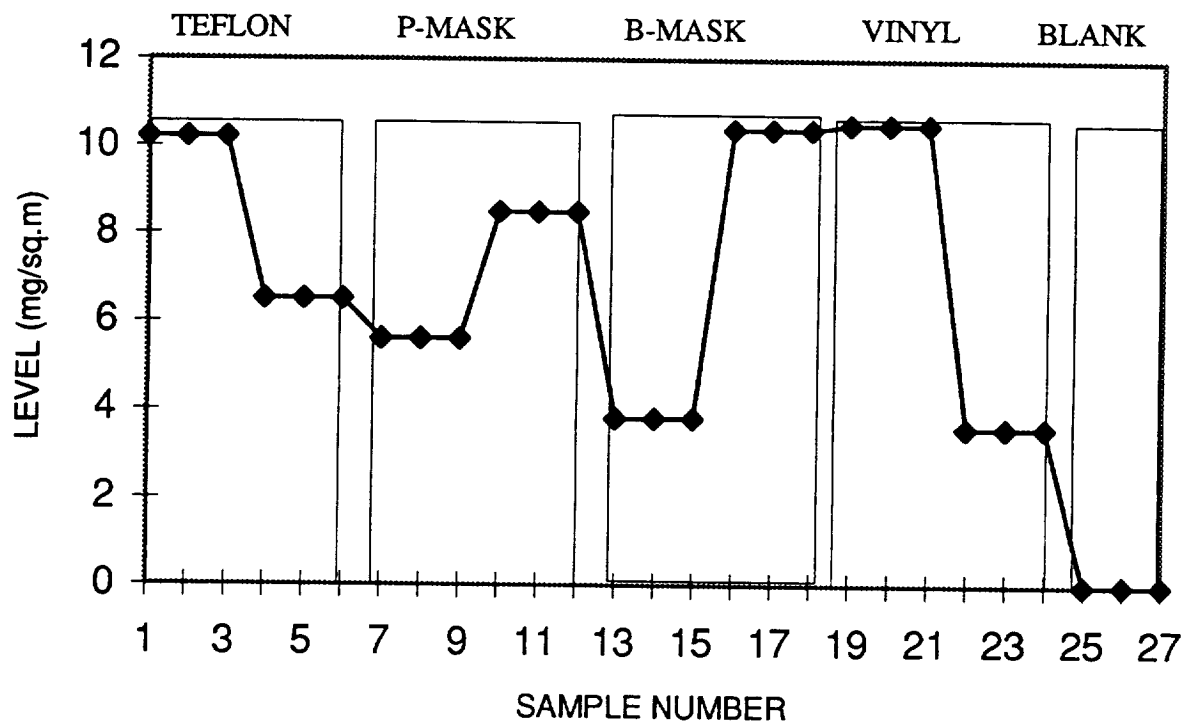
The residues of adhesives from four different tapes used by Thiokol in their manufacturing process were studied in this experiment. Data was collected from the residue that might remain on a bonding surface after tape has been applied, then removed and the adhesive cleaned from the surface. The residues from four different tapes currently used by Thiokol were extracted using 1,1,1 Trichlorethane as a solvent. The four tapes studied, and their occurrence in the manufacturing process, are

- 1) Teflon tape, a tape used in the grit blast process;
- 2) P mask, a masking used in the painting operation;
- 3) B mask, a masking used in the grit blast process;
- 4) Vinyl tape, a tape used in the cleaning operation.

The residues were sprayed concurrently on large aluminum plates and witness foils. The gravimetric weights were determined for the witness foils from which conclusions about the levels

on plates were deduced. Each residue was applied in two distinct levels of contamination, yielding eight contaminated levels, two for each type of contaminant. A blank panel was prepared to provide a zero reference for the study. Figure 1 provides an ordering of the contamination levels sprayed on the panels. This ordering is important for the interpretation of the loadings and scores plots. Spectral data for three different spots over each contaminated level were taken and recorded. Also, three different spots were scanned on the blank panel.

Figure 1. Distribution and ordering of residue levels within the sample matrix



Spectral data was taken using the 9-10 optical fiber probe to illuminate and to receive with the Guided Wave 260 after the plates had been contaminated. Scanning parameters were set according to the following:

- Spectral Averages            1
- Point Averages                5
- Dwell Degrees                0 cycles
- Wavelength                    1.1  $\mu\text{m}$  to 2.2  $\mu\text{m}$  step 1.0  $\mu\text{m}$
- Detector                        Germanium with .25 slit, 1.1  $\mu\text{m}$  to 1.6  $\mu\text{m}$   
                                       PbS with 1.0 slit, 1.6  $\mu\text{m}$  to 2.2  $\mu\text{m}$

The data was then subtracted from a gold reference scan using SpectraCalc, smoothed, and exported to a format which then could be compiled through the exported data to the Unscrambler format for PLS1 and PLS2 analyses. Results for the PLS1 models are presented in Figures 2 through 7. Figures 2 and 3 show the loadings and scores of factor 1 for the residue from the teflon tape. The loadings do resemble spectra rich in OH and CH bands.

Figure 2. Loading of factor 1 for the teflon tape.

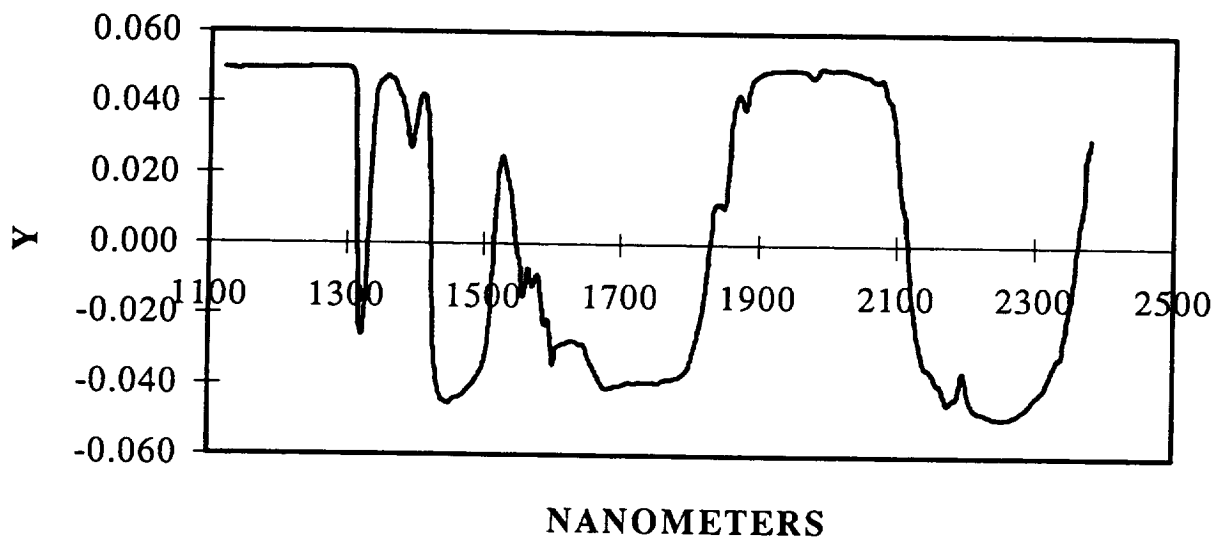
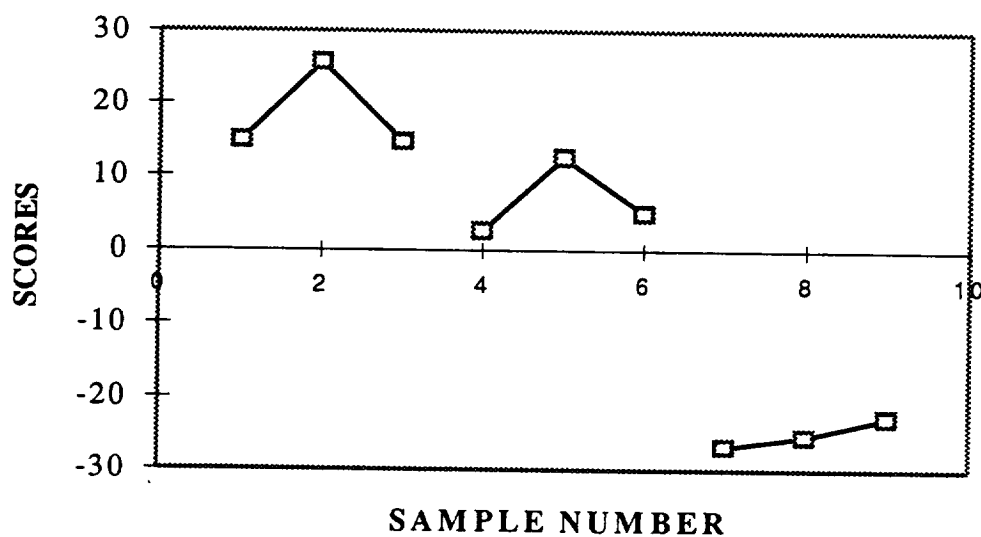


Figure 3. Scores for the teflon tape residue



Factor 1 includes 94% of the variance in Y, which implies that the loading will have a high correlation with the actual spectrum of the species contained in the residue. The loading appears to be the negative of the actual spectrum and this is due to a reversal in sign during the matrix decomposition. The scores plot indicates that there are differences in the three observed spectra for a given level of contamination on the panel. However, for reporting purposes an average of the three points yields a value for each contamination level very near the value determined by the gravimetric method. Figures 4 - 9 show the loadings and scores for the other three residues included in this report. There are noticeable differences in the spectra.

Figure 4. Loadings for P-mask residue.

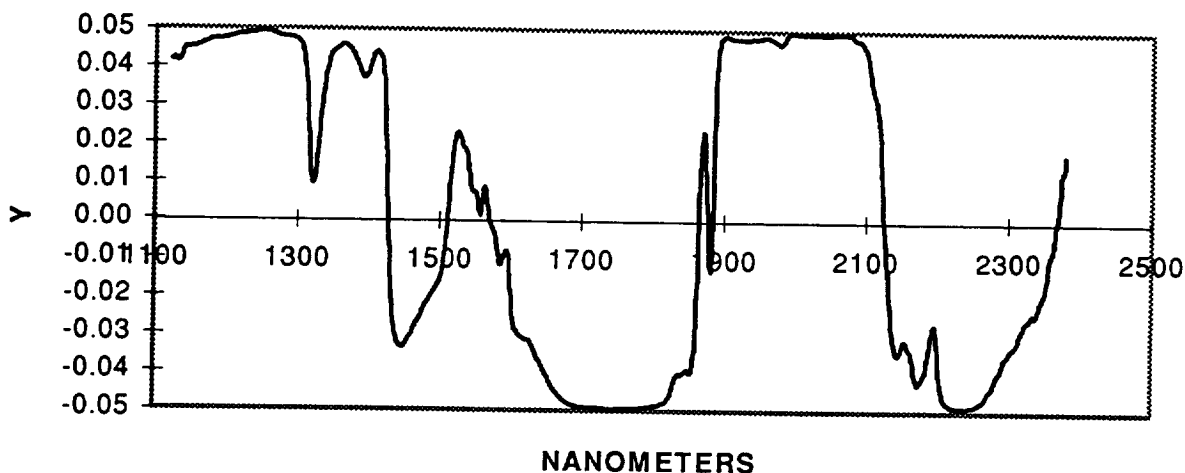


Figure 5. Scores plot for the P-mask residue

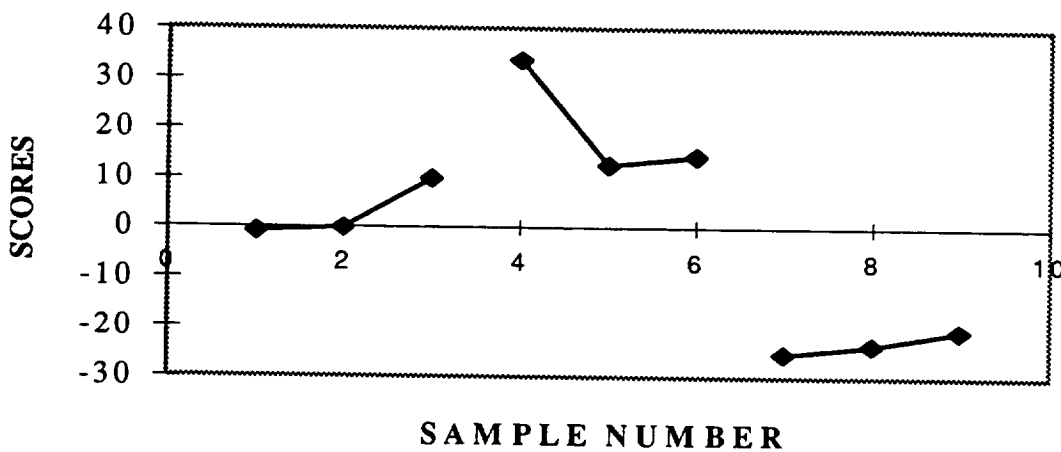


Figure 6. Loadings plot for B-mask tape residue.

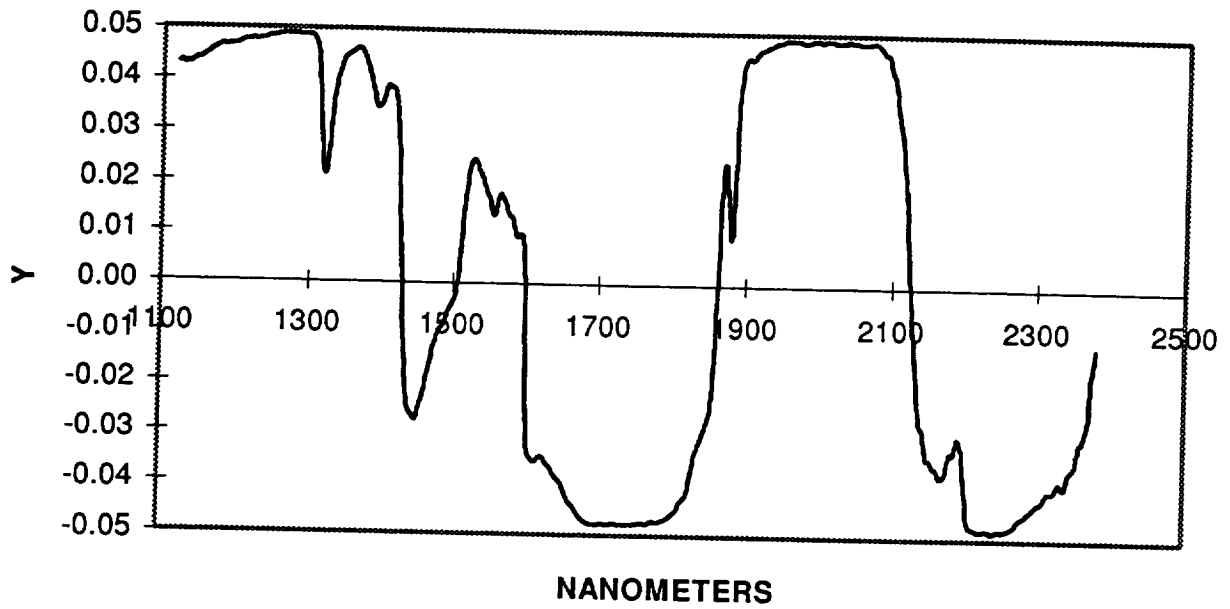
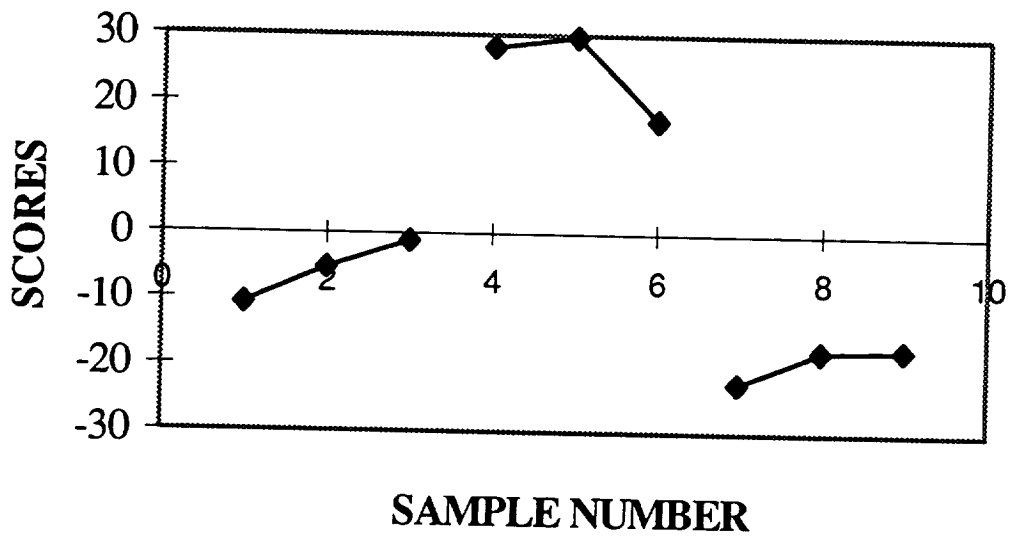
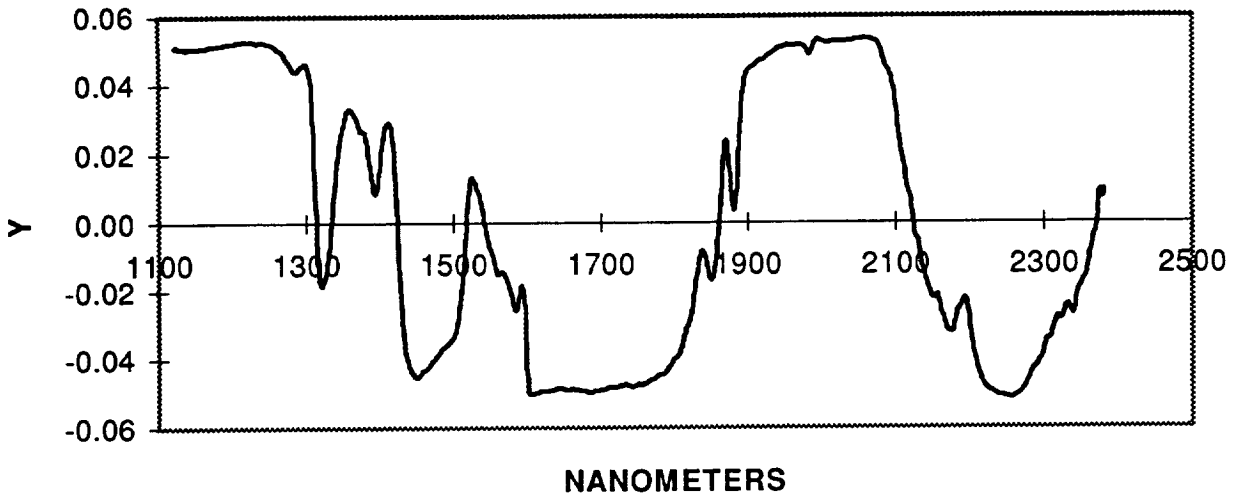


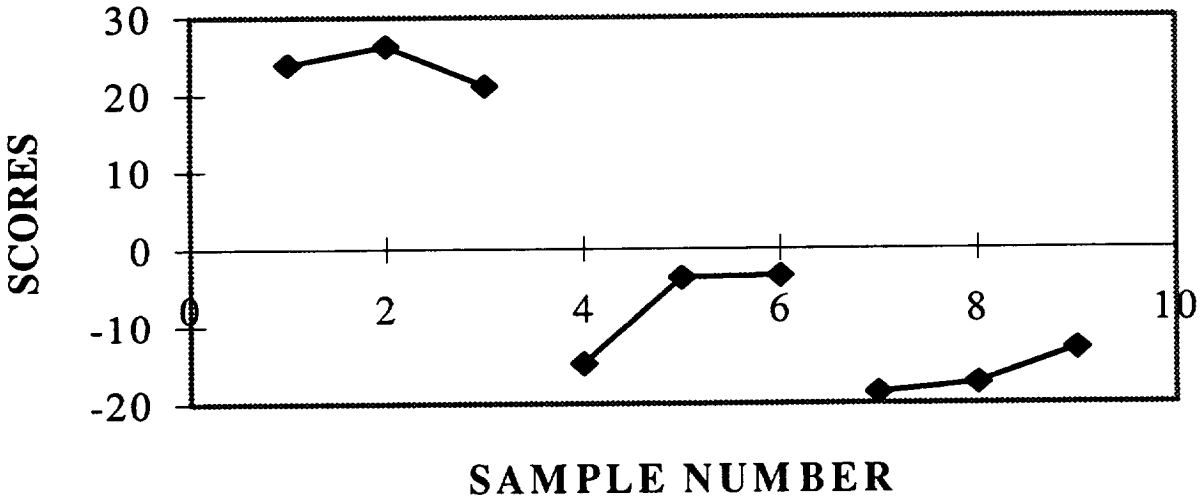
Figure 7. Scores for B-Mask tape residue



**Figure 8. Loadings for Vinyl Residue**



**Figure 9. Scores plot for Vinyl Adhesive**



A PLS2 analysis was performed on the spectral data to determine the predicted contamination levels of each residue. The PLS2 model included all the data from all the contaminated panels. This model was then used to predict the individual contamination levels for each different residue as if they were unknown. In other words the model contained all the variation present in the set of known residues on the panels. This information is then used to

predict a single residue signature using the significant factors identified in the PLS2 model. The numerical results are listed in Table 1 below.

TABLE 1. Numerical Results for residue PLS2 Analysis

SAMPLE	TEFLON		P MASK		B MASK		VINYL	
	Y-PRED	DEV	Y-PRED	DEV	Y-PRED	DEV	Y-PRED	DEV
1	10.15	1.41	-0.13	2.25	0.10	1.43	0.08	1.30
2	6.33	1.37	0.24	2.18	0.01	1.39	0.00	1.26
3	0.20	1.37	5.30	2.19	-0.07	1.39	-0.24	1.27
4	-0.11	1.41	8.39	2.25	0.24	1.43	0.19	1.30
5	0.23	1.27	0.21	2.02	3.71	1.28	0.34	1.17
6	0.02	1.38	0.08	2.21	9.86	1.40	-0.02	1.29
7	0.19	1.41	0.13	2.26	-0.24	1.43	10.22	1.31
8	-0.33	1.32	-0.29	2.11	0.99	1.34	3.36	1.22
9	0.042	1.37	0.18	2.19	-0.40	1.39	0.17	1.27

A useful indicator of how well the model fits the observations is determined by the correlation coefficient between the model and the data and the by comparing the predicted values of the regression model with the actual values. Figures 10 - 13 show the plots of the predicted values versus the measured values. The correlation is very high even for the few points used in generating the model. It is noteworthy that to get the tight correlation shown that 15 factors were necessary as well as averaging the three points for each contamination level. The results have shown also that simple averaging of the observations for each unknown sample, which is a common measurement process in practice, provides very good statistical fit of the observations to the predicted results.

Figure 10. Predicted versus Measured Values for Teflon Tape

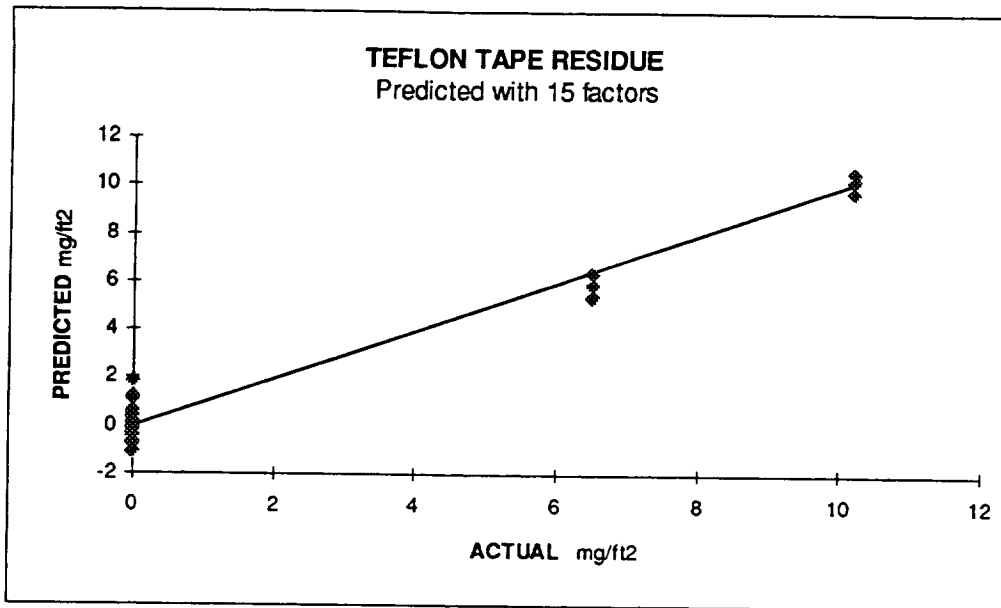
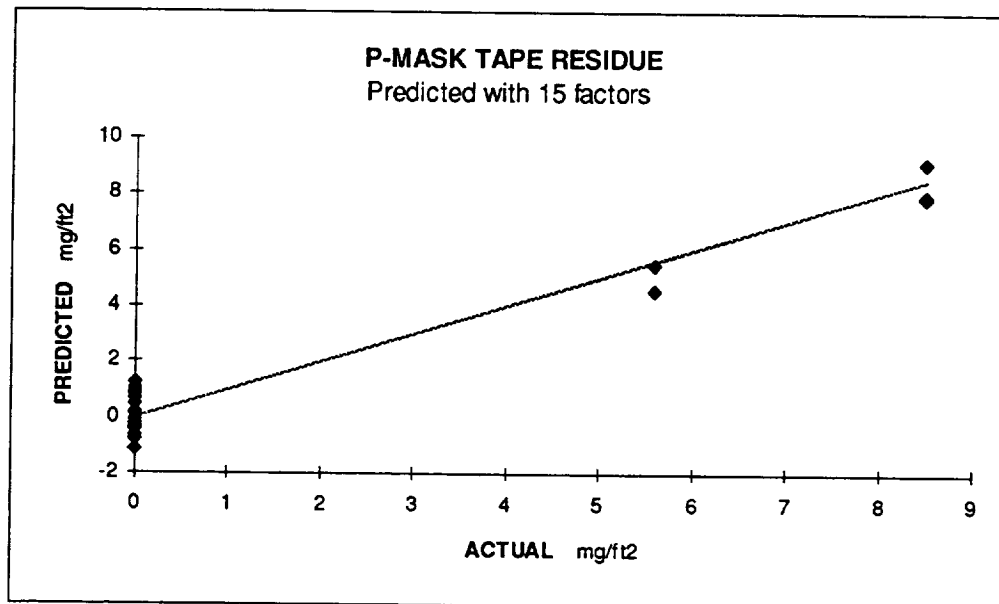
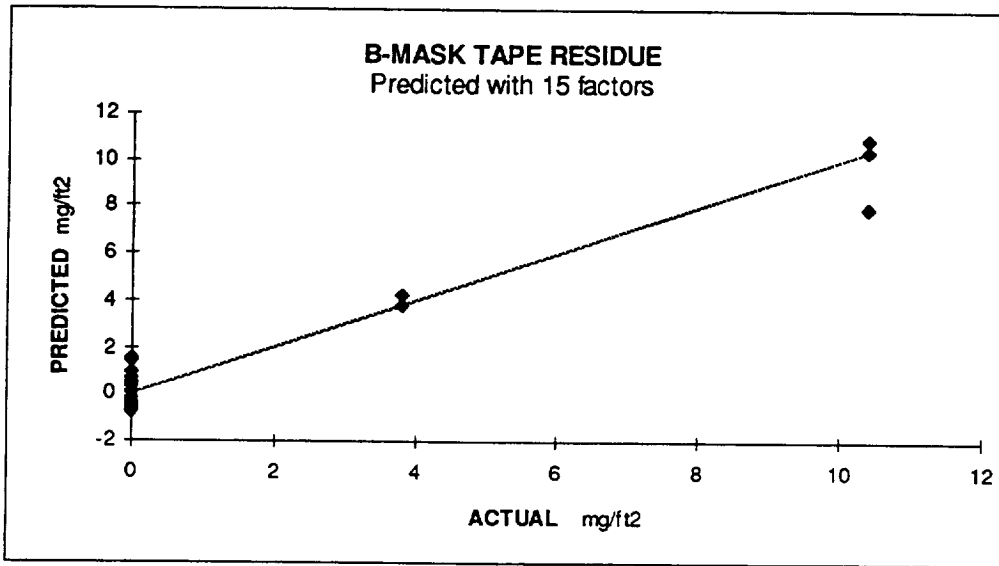


Figure 11. Predicted versus Measured Values for P-Mask Tape

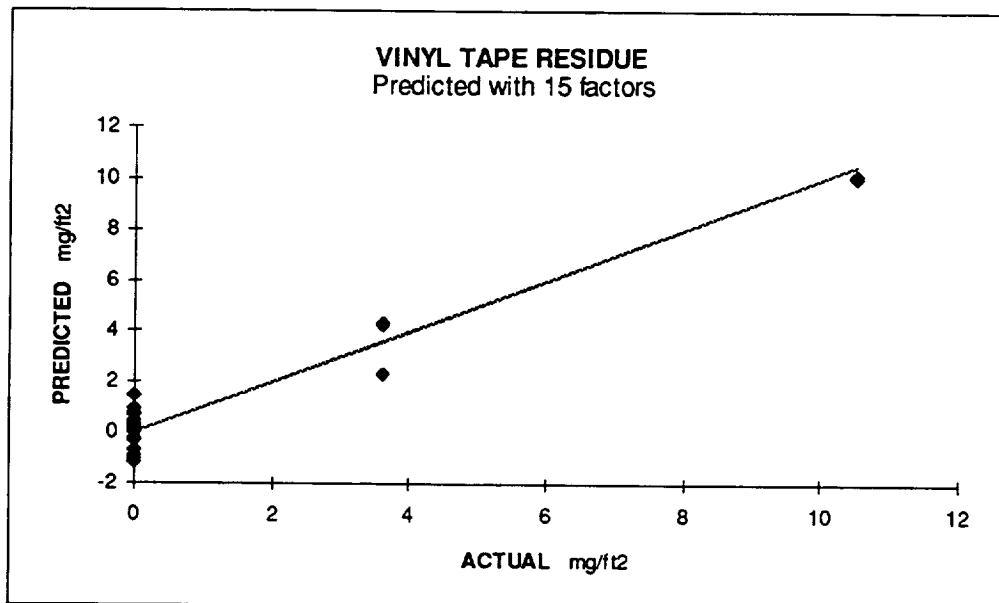




**Figure 12. Predicted versus Measured Values for Teflon**



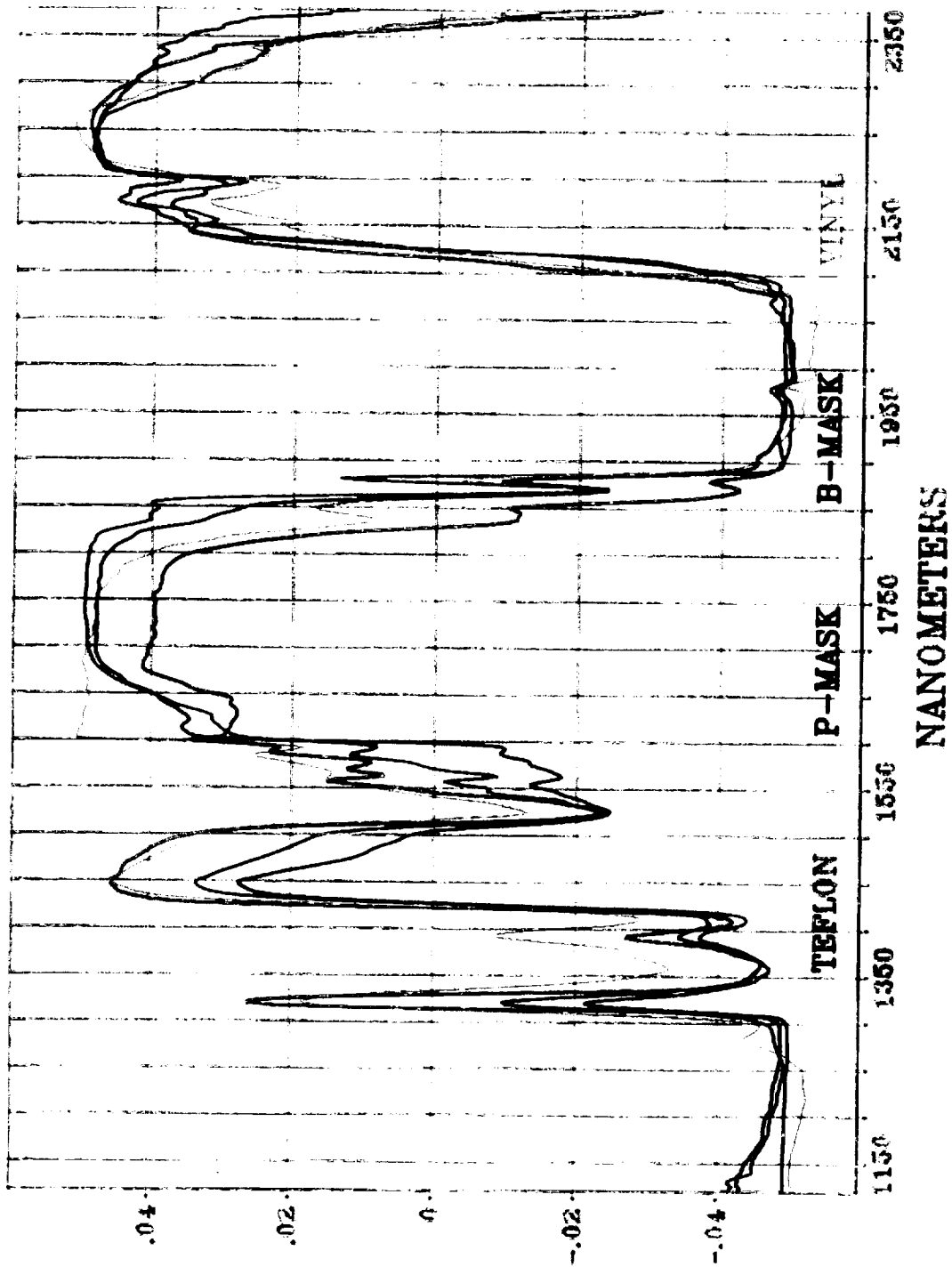
**Figure 13. Predicted versus Measured Values for Vinyl Tape**



The conclusion can be made that the NIR spectra can be used to separate out the four different residues of the tapes in this study using partial least squares analysis and thereby yield quantitative data as well as qualitative data. It is doubtful that mid-IR data would have given as good results, since the NIR spectral region has many more feature variations to work with in differentiating between the four adhesives. This data was smoothed in an attempt to provide spectral features which are more readily understood by the spectroscopist. However, if the spectral bands are not needed for manual identification purposes, then the data would yield better quantitative results using fewer factors if not smoothed prior to PLS2 or PLR analysis. This is because the smoothing routines probably remove some of the variation the multivariate approach relies on for identification confirmation.

Some effort has been made in making line assignments using the loadings for the first factor for each residue. These loadings are compared with IR transmission spectra for each residue respectively. Figure 14 shows the overlaid loadings of all tape residues showing the similarities and the areas of the spectra which are different. We were unable to obtain the transmission IR spectra data directly from the Nicolet instrumentation at MSFC because it was saved as a library file and not as a spectral file. It would be necessary to obtain new transmission data in the IR to proceed with line matching in the NIR region.

Figure 14. Overlay of the First Factor for All Four residues.



TAPE RESIDUES FIRST FACTOR X -1

## 7.0 Integrating sphere precision test:

Additional tests were run to determine if spectroscopic measurements performed using an integrating sphere might provide a more precise measurement on SRM surfaces. Part of the reasoning behind this sequence of measurements lies in the occurrence of diffuse scattering from the types of surfaces encountered in most surfaces which are not optical reflecters, such as mirrors. The optical fibers currently being used show a strong influence on the nature of the scattered radiation from these diffuse surface features. Some processing schemes, such as described with the MSC approach, do alleviate some of these problems with real surfaces. However, it is still worth the effort to eliminate as many physical factors as possible in obtaining spectral measurements from the surfaces being inspected. In this way, the integrating sphere provides a useful approach to utilizing a larger percentage of the diffuse rays being emitted from the surface of the sample and launching them into the optical fiber leading back to the spectrometer.

The test surfaces were D6AC steel substrates contaminated with HD2 grease and silicone in varying concentrations of 1" strips across a 6" by 6" plates. The integrating sphere used in this preliminary study was originally purchased for operation in the UV region; however, the coating materials did not prevent usage in the NIR. The sphere parameters were:

- Diameter of diffuse surface - 6" .
- Sample port diameter - 2"
- Detector port - 9-10 probe attached at 25° from sample port
- NIR source port - Unisource 6000 fiber bundle at 45° from sample port

Spectrometer parameters:

- Scan range - 1  $\mu\text{m}$  to 1.6  $\mu\text{m}$
- Spectral averages - 1
- Point averages - 5
- Dwell - 0
- Detector used - Germanium with .5 slit and 300 l/mm grating

Scans of the contaminated plates were accomplished by performing complete scans over the same spot on the plate for five complete spectra. This was repeated for three different levels of average contamination on each plate. With the sample port diameter of 2" and different

contamination levels every 1" across the plate, it was necessary to average the levels of two bands for the known contamination level. Standoff distance from the sample port to the surface of the plate measured normal to the plate surface was 0.5".

The spectral data was first subtracted from a Au reference using Spectra Calc to obtain absorbances. No smoothing of these spectra was performed. This data was then compiled into an Unscrambler file for multivariate analysis. The procedure used was to generate the model about the mean with PLS2 and cross correlation. A plot of predicted vs. measured was made and is shown in Figures 15 and 16.

The correlation of the data using eight factors gave correlations of better than .99 for both the HD2 grease and the silicone contamination. The graphs indicate that the average spectra for even as few measurements made here, can provide very quantitative and reliable information on contamination levels. Note that the cluster of data points at 0 represents those samples having no contamination, i.e. blanks.

**Figure 15. Plot of Predicted versus Measured Values for HD2 Grease using an Integrating Sphere**

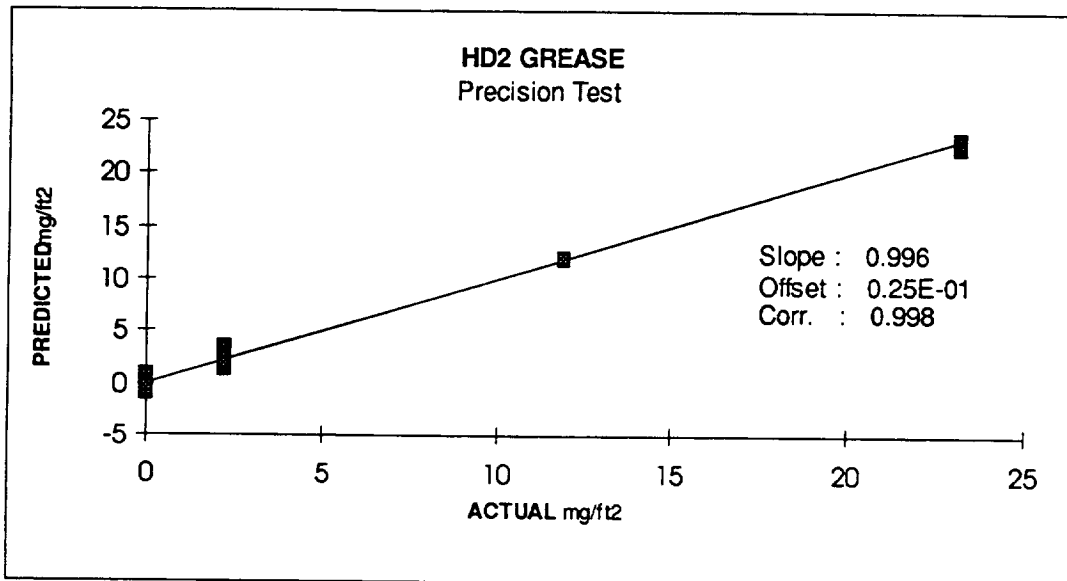
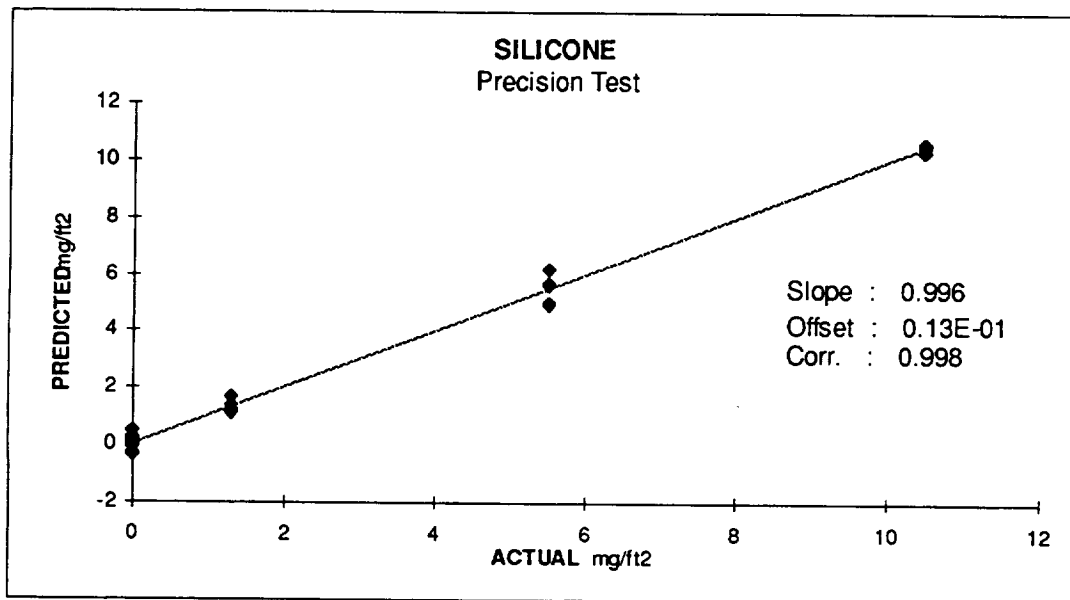


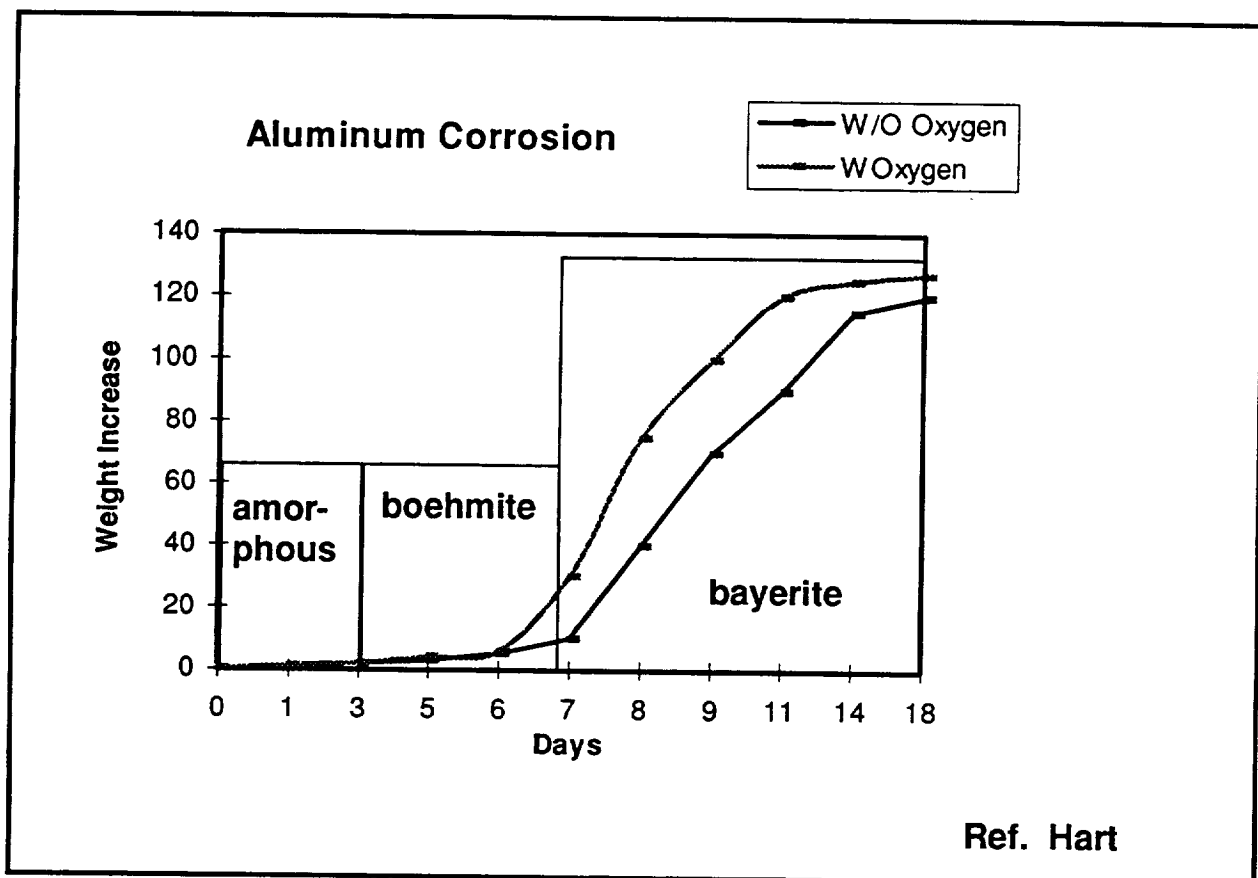
**Figure 16. Plot of Predicted versus Measured Values for Silicone Grease using an Integrating Sphere**



## 8.0 Spectra for 7075 Al for aluminum hydroxide identification

Historically, a lot of experimentation has been performed in trying to determine and characterize the types of oxide/hydroxides which form on aluminum surfaces. This surface chemistry is very important in trying to understand what bonds can form on such surfaces and how to measure the ability of the surface to form bonds and or corrode in a humid environment. The early work by Alwick [3] and Hart [7] identified the stages at which the various forms of aluminum hydroxide occur during oxidation/hydrolysis in the presence of moisture at ambient temperatures. For example, figure 17 shows the two stages of hydroxide formation occurring on an aluminum surface immersed in an aqueous bath with and without oxygen aeration. Note that an initial film of pseudo-boehmite forms which slowly changes over to bayerite, even at ambient temperatures.

Figure 17. Rate of hydroxide formation on immersed aluminum surface at ambient temperatures.



The surface for this test was prepared as follows: A 7075 aluminum coupon was polished by use of a polishing disk using progressively finer grit media to obtain a clean and fresh surface.

The coupon was then immediately immersed in a distilled deionized water bath. The coupon was removed from the bath and dried with nitrogen after 24 hours of aging. The coupon was then used for data acquisition on the Woolam ellipsometry system at MSFC. It was then allowed to further age in ambient atmosphere for a period of one month before this test was performed. The expected result was two films; a robust film of bayerite on a thin film of aluminum oxide.

Spectrometer parameters:

Scan range - 0.63  $\mu\text{m}$  to 0.97  $\mu\text{m}$  and 1.0  $\mu\text{m}$  to 1.6  $\mu\text{m}$

Spectral averages - 1

Point Averages - 5

Dwell -0

Detectors used - 0.63  $\mu\text{m}$  to 0.97  $\mu\text{m}$ ; Silicone with 0.25 slit

1.0  $\mu\text{m}$  to 1.6  $\mu\text{m}$ ; Germanium and Lead Sulfide with 0.25 slit

NIR spectra were obtained by scanning the same area with the 9-10 probe for 20 repeated scans in each spectral range. Data was subtracted from a gold reference using Spectra Calc. Smoothing was performed on each spectra by using Savitsky-Golay 9 point smooth followed by a Savitsky- Golay 5 point smooth. Data was then compiled into an Unscrambler file for multivariate analysis. The PLS1 model about the mean with cross validation was used for the analysis. The PLS1 model is reported; however, as a check a PCA model was also performed and the two approaches agreed with each other in both the scores and loadings.

Once again the results of the PLS analysis is determined to be valid once the variances for both the X variables and the Y variables are primarily accounted for and the loadings are reasonably close to spectral features. Usually the spectral features can be explained for known OH and CH peaks using second and third harmonics and combination bands. The following results from the PLS analysis does show that statistical analysis does provide reasonable results.



**Figure 18. Plot of Per Cent X Variation accounted for in 7075 Aluminium Experiments - 0.635  $\mu\text{m}$  to 0.935  $\mu\text{m}$**

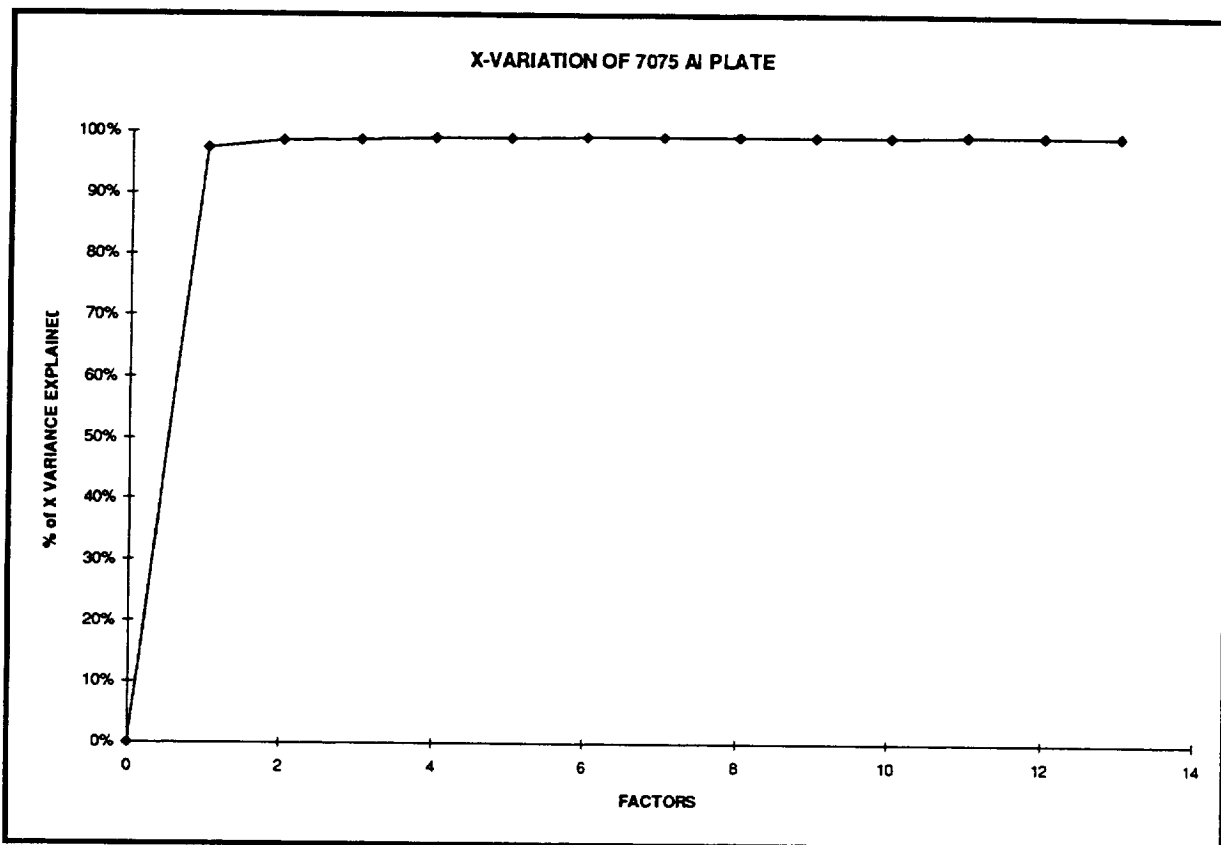


**Figure 19. Plot of Scores for Factor 1 with no Outliers Removed in 7075 Aluminium Experiments - 0.635  $\mu\text{m}$  to 0.935  $\mu\text{m}$**

Figure 18 indicates that the X variance is 98% explained in the first two factors. In figures 19 and 20 on the following page, it is seen that factor one shows increasing factors and has a loading which gives several spectral features. In figure 20 it is also noticed that the bands at 872 nm and 882 nm look very close to the bayerite spectra in the mid-IR given by Wefers and Misra[2]. The other features around the 746 nm band are probably water overtones. Figures 21 and 22 do not account for much of the variation in the spectra set, but it is noted that the loading for factor two appears to be inverted features of factor one.

Figure 20. Plot of Scores for Factor 1 with No Outliers Removed in 7075 Aluminium Experiments - 0.635  $\mu\text{m}$  to 0.935  $\mu\text{m}$

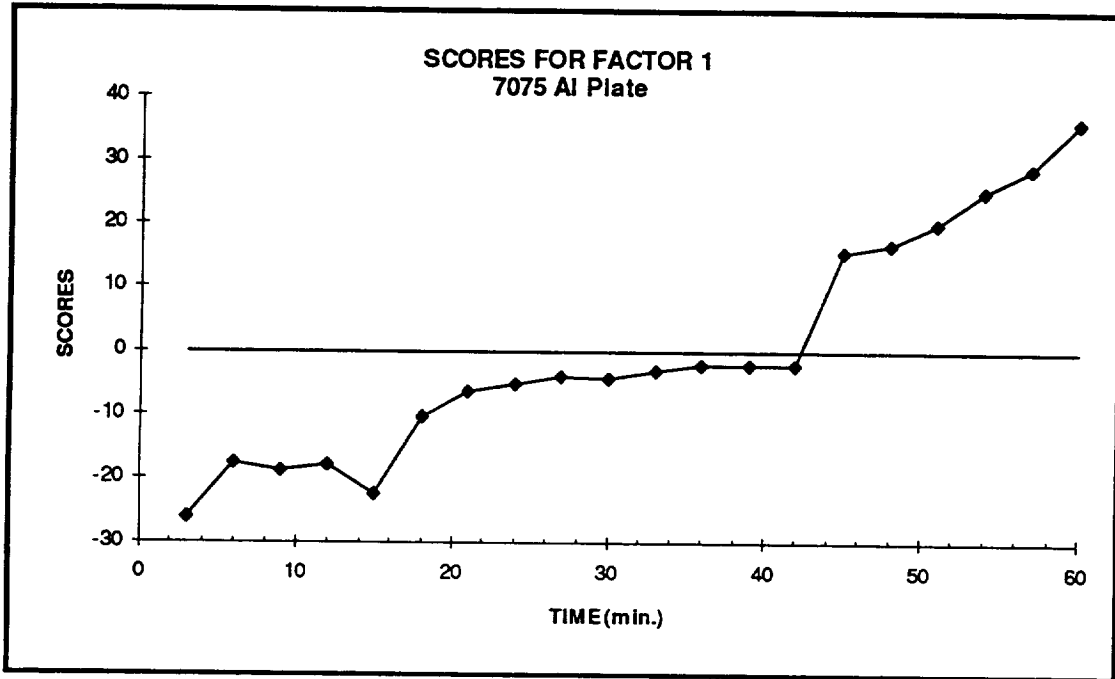


Figure 20. Plot of Loadings for Factor 1 with No Outliers Removed in 7075 Aluminium Experiments - 0.635  $\mu\text{m}$  to 0.935  $\mu\text{m}$

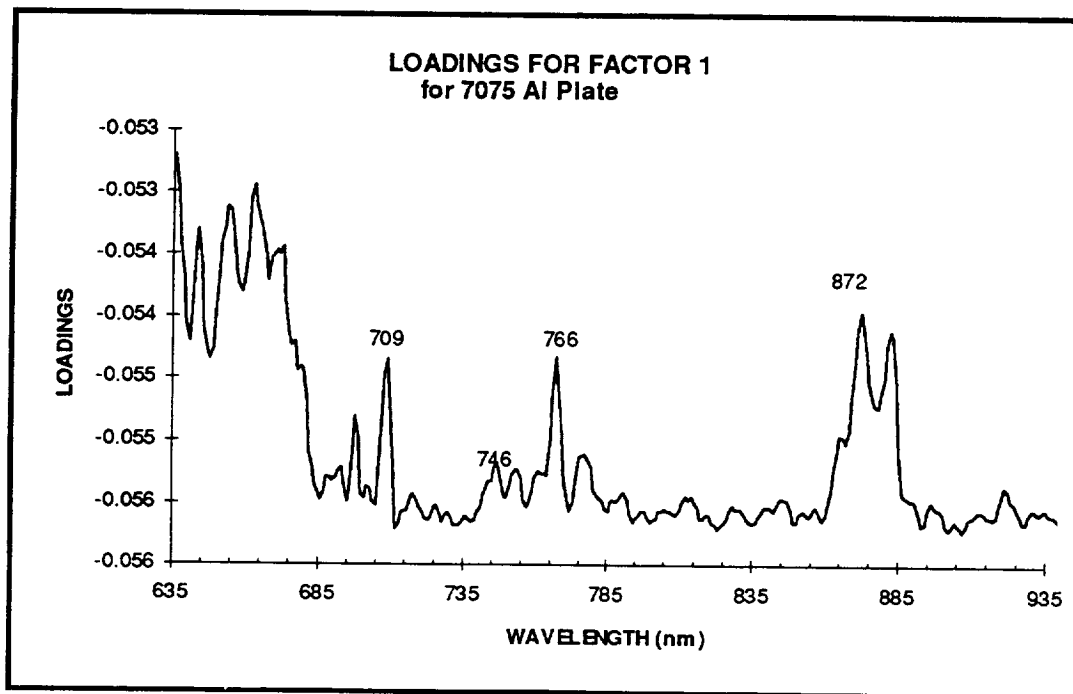


Figure 21. Plot of Scores for Factor 2 with no Outliers Removed in 7075 Aluminium Experiments - 0.635  $\mu\text{m}$  to 0.935  $\mu\text{m}$

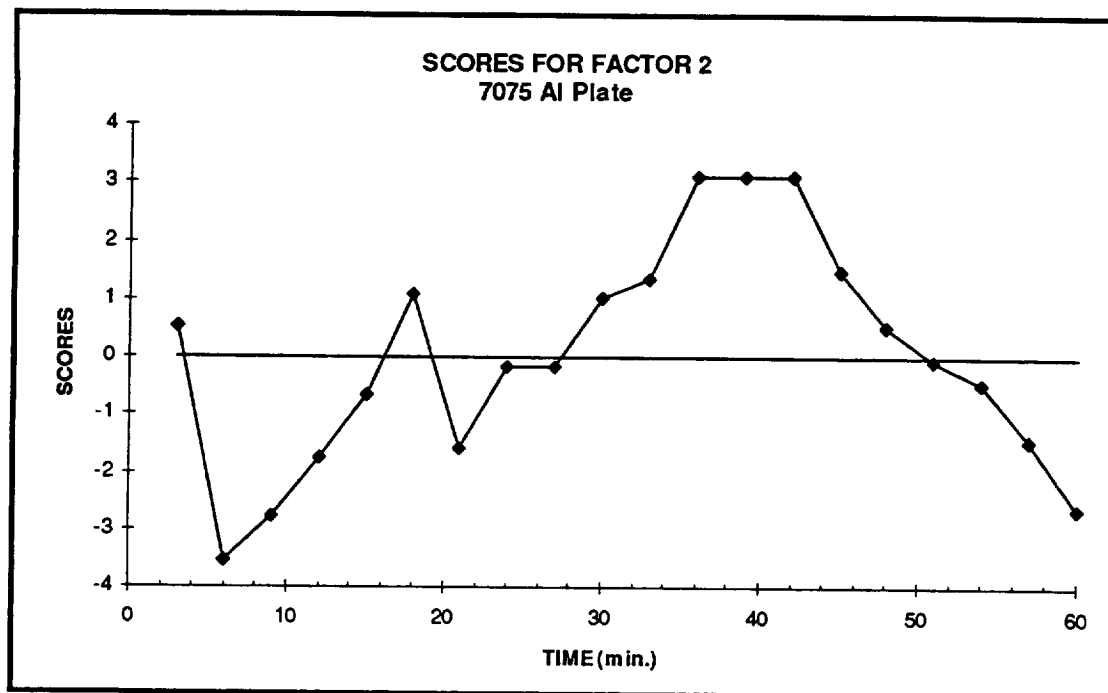
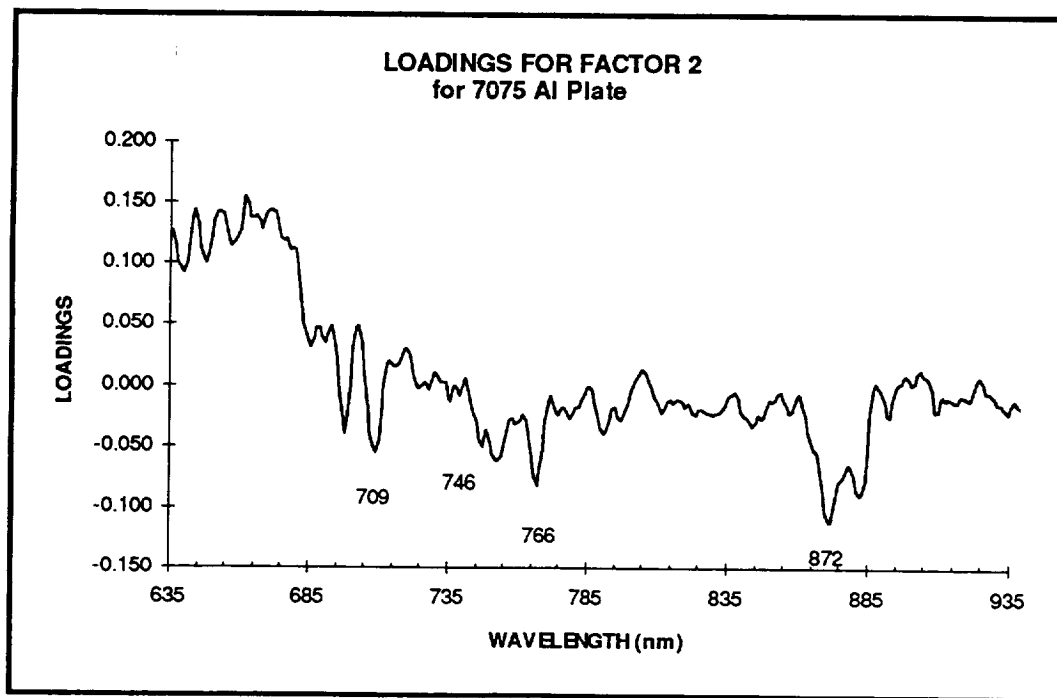


Figure 22. Plot of Loadings for Factor 2 with no Outliers Removed in 7075 Aluminium Experiments - 0.635  $\mu\text{m}$  to 0.935  $\mu\text{m}$



Spectra of the 1.0 to 1.6  $\mu\text{m}$  range was taken as a comparison with spectra we had seen in past experiments. Figure 23 gives the X variance explained as a function of factor number and it shows that only 90% is explained in the first two factors. Figures 24 and 25 then give the scores and loadings for the first factor. This set had to be reduced because of outliers in the data. Again a trend towards a growth of factor one is shown and the spectral features look similar to past data taken on 7075 Al plates with hydroxide layers present. There is also the predominant water band and other features which might be due to the -OH bonding to the Al atoms.

Figure 23. Plot of Per Cent X Variation accounted for in 7075 Aluminium Experiments for 1 $\mu\text{m}$  to 2 $\mu\text{m}$  Wavelengths

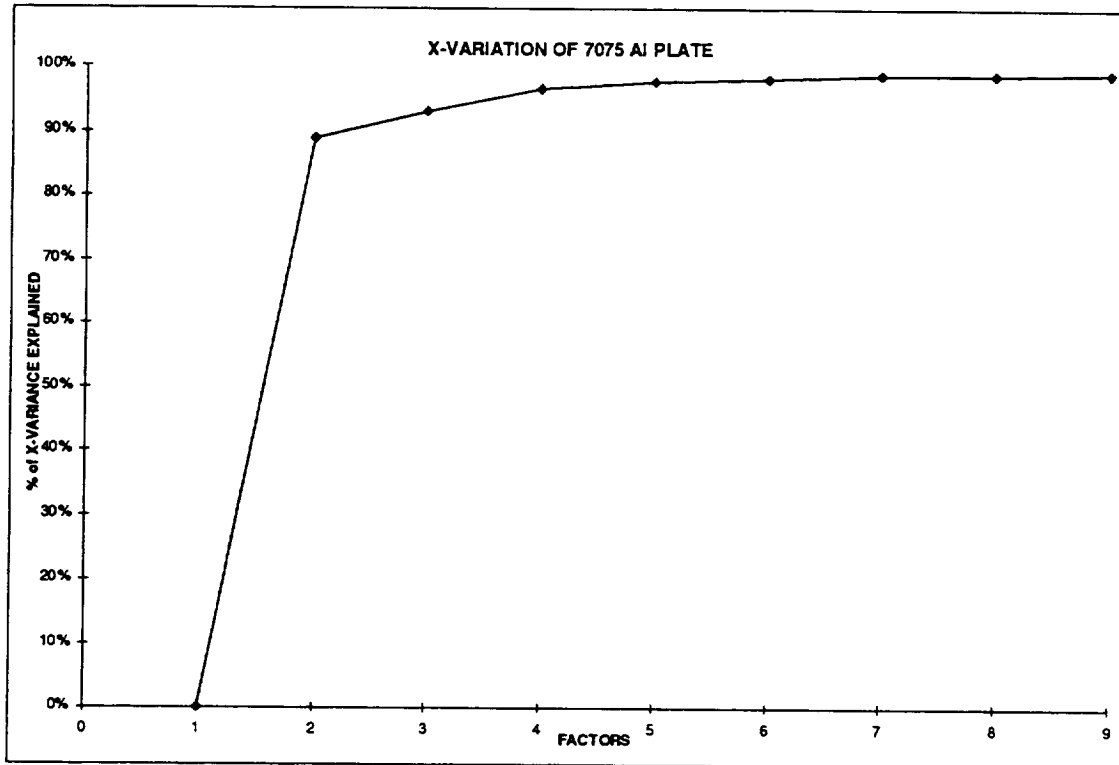


Figure 24. Plot of Scores for Factor 1 with Outliers removed in 7075 Aluminium Experiments - 1.1 $\mu$ m to 1.6  $\mu$ m

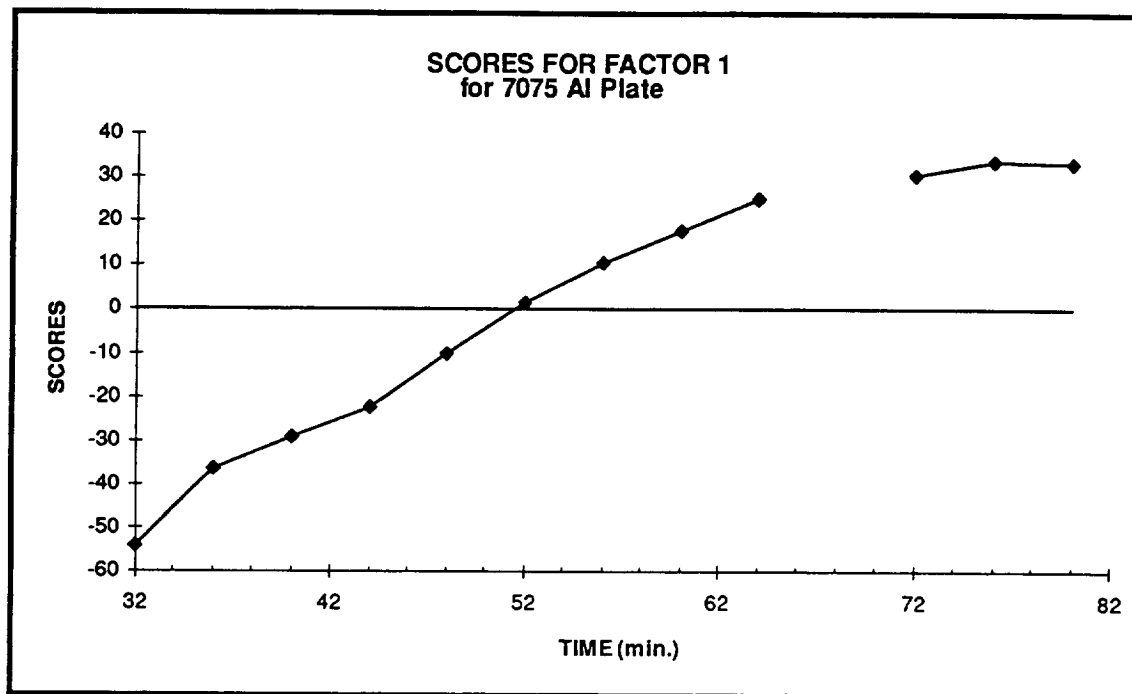
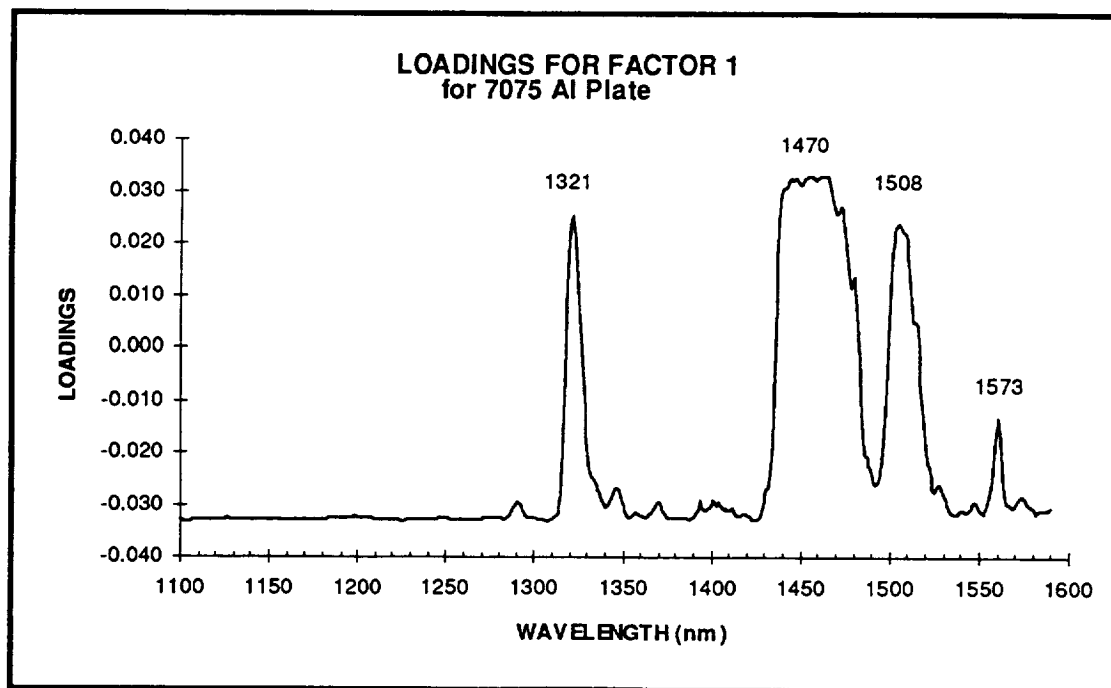
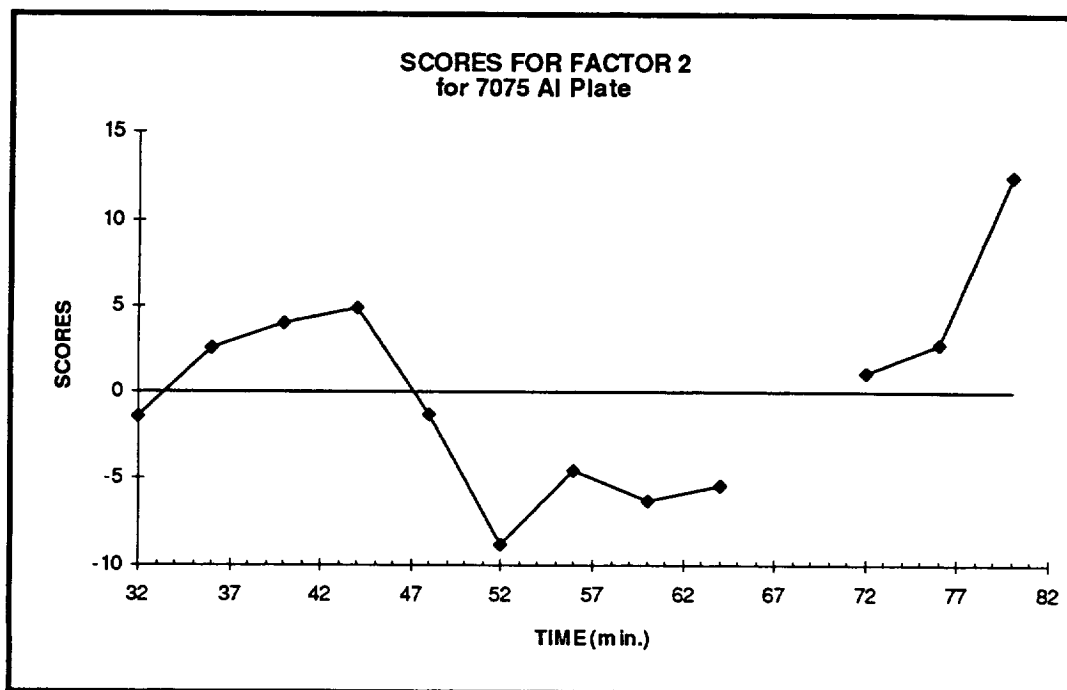


Figure 25. Plot of Loadings for Factor 1 with Outliers Removed in 7075 Aluminium Experiments - 1.1  $\mu$ m to 1.6  $\mu$ m

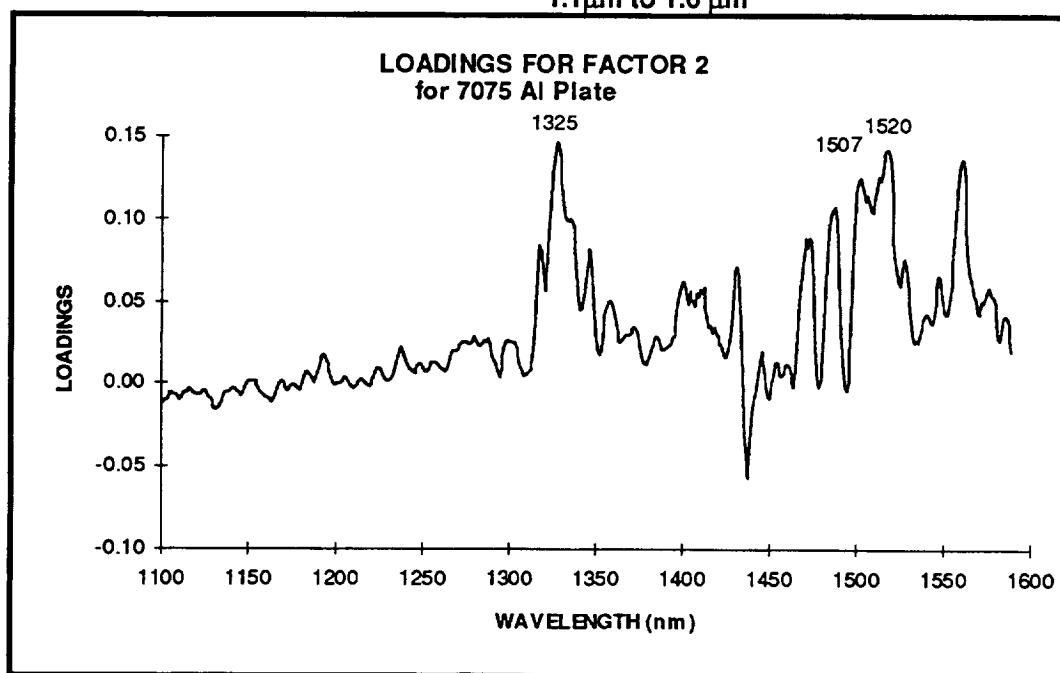


Figures 26 and 27 likewise give scores and loadings for factor two.

**Figure 26. Plot of Scores for Factor 2 with Outliers Removed in 7075 Aluminium Experiments - 1.1  $\mu\text{m}$  to 1.6  $\mu\text{m}$**



**Figure 27. Plot of Loadings for Factor 2 with Outliers Removed in 7075 Aluminium Experiments - 1.1  $\mu\text{m}$  to 1.6  $\mu\text{m}$**



## 9.0 Comparison of NIR Spectra and Ellipsometry on NIST Al Mirror

An aluminum front surface mirror standard certified by NIST was obtained from EH laboratory at Marshall Space Flight Center in order to better characterize the surface chemistry of aluminum. The mirror is two inches in diameter and coated with SiO to protect the surface from scratches. It was not apparent at this time how the SiO affects the surface chemistry.

Spectrometer parameters used for this sequence were:

Scan range - 0.65  $\mu\text{m}$  to 0.97  $\mu\text{m}$

Spectral averages - 1

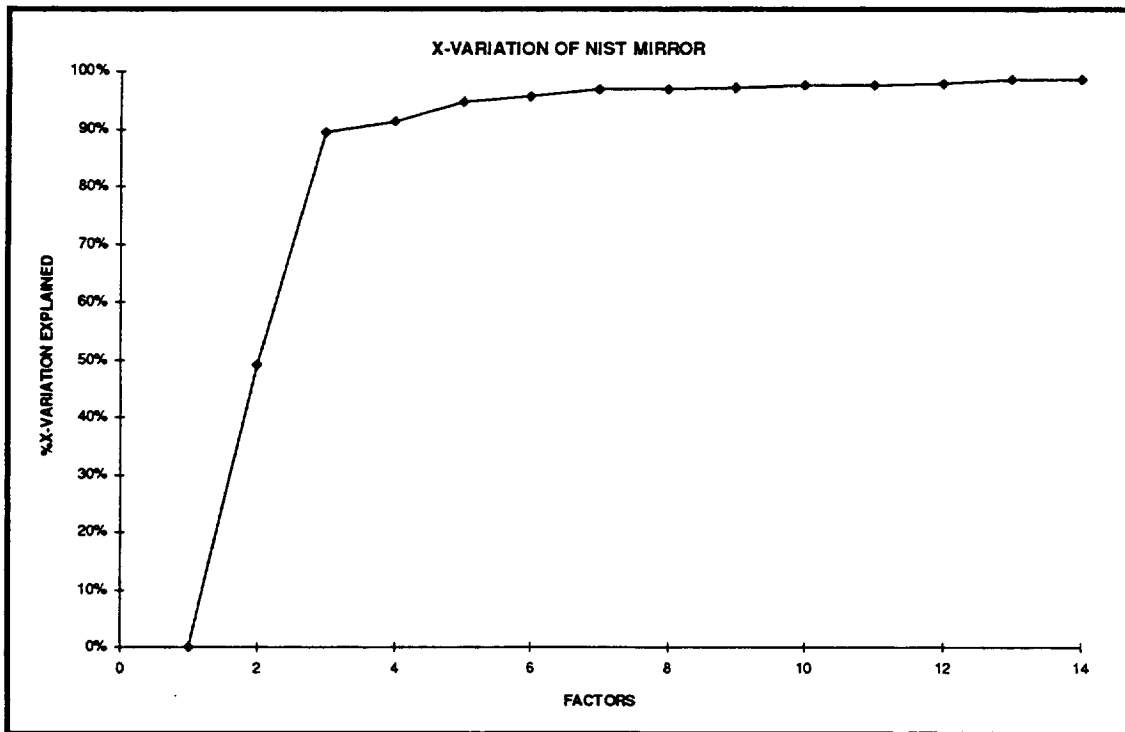
Point Averages - 5

Dwell - 0

Detector used - 0.63  $\mu\text{m}$  to 0.97  $\mu\text{m}$ ; Silicone with 0.25 slit

Spectra were obtained by scanning the same area with the 9-10 probe for 20 repeated scans in the spectral range given. The scan period chosen for this study was 4 min. and 30 sec. Spectral data was prepared as described earlier for the aluminum hydroxide study. Figure 28 shows that the X variance of 92% was explained in two factors.

Figure 28. Plot of Per Cent X Variation for NIST Mirror Standard for 0.635  $\mu\text{m}$  to 0.935  $\mu\text{m}$



Figures 29 and 30 show the scores and loadings for factor one. Comparing the loading of the mirrors first factor with the first factor loading of the 7075 aluminum plate we notice the absence of most of the spectral features that were present on the 7075 aluminum plate. It appears that the mirror has one large water band and the scores indicate that it is increasing as the scans repeat with time.

**Figure 29. Plot of Scores for Factor 1 for NIST Mirror Standard - 0.635  $\mu\text{m}$  to 0.935  $\mu\text{m}$**

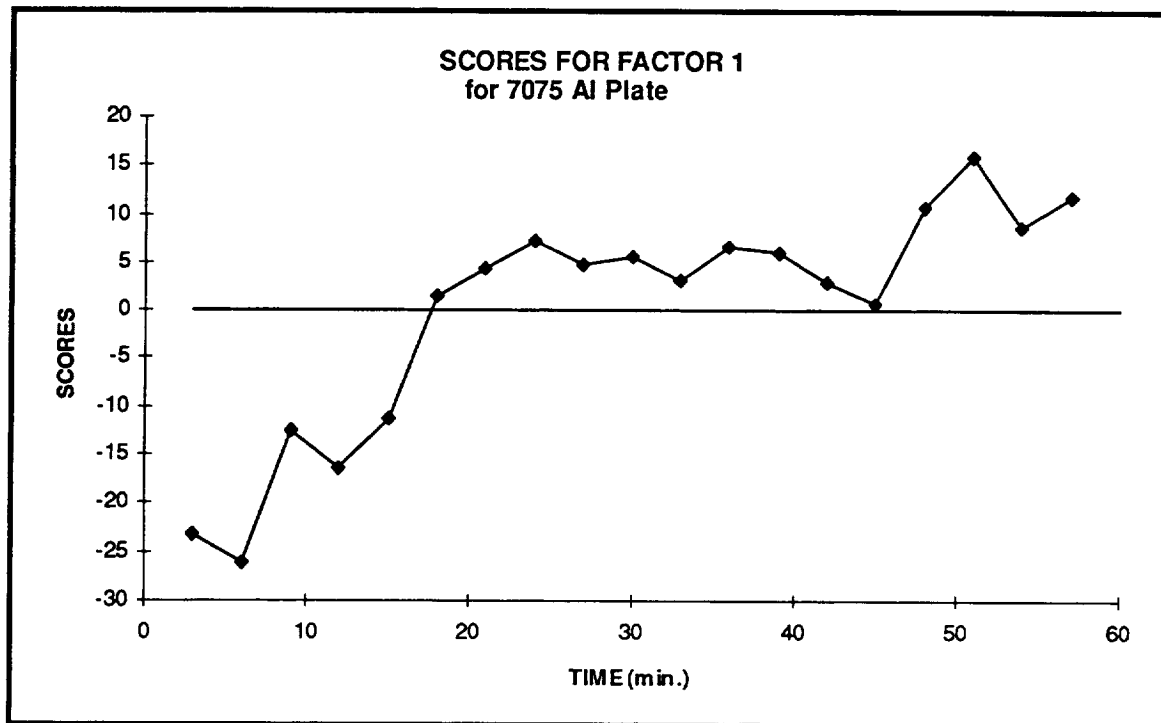
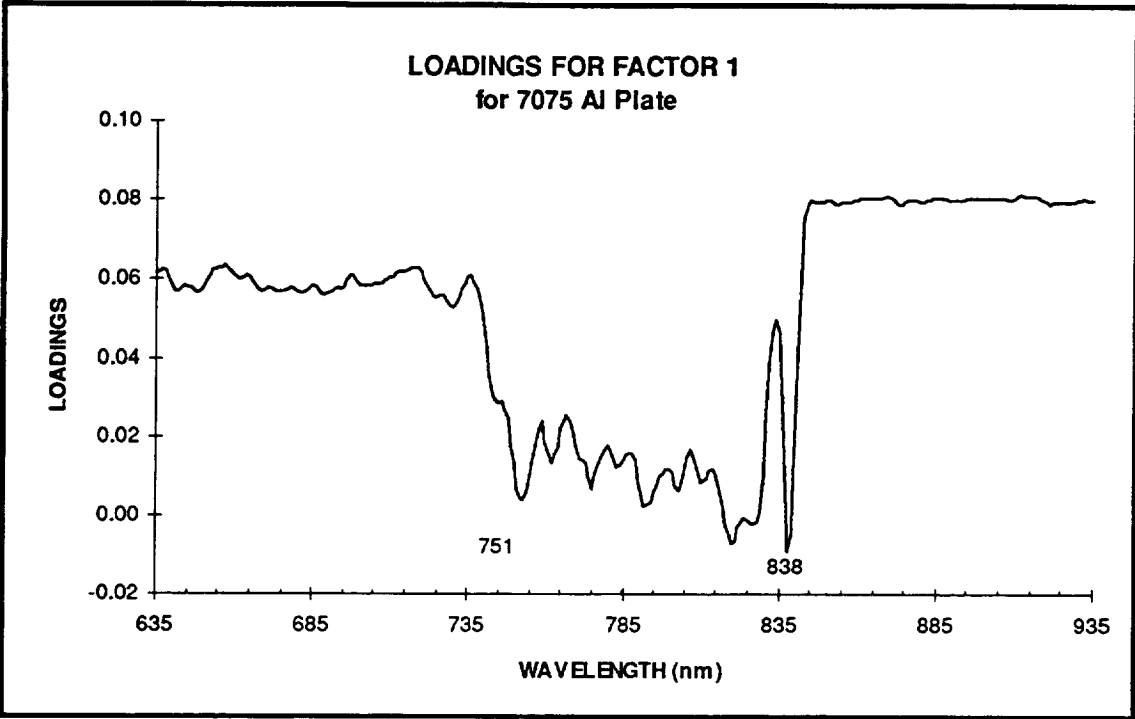




Figure 30. Plot of Loadings Factor 1 for NIST Mirror Standard - 0.635  $\mu\text{m}$  to 0.935  $\mu\text{m}$



Likewise figures 31 and 32 give the scores and loadings for factor two of the mirror with little information present.

Figure 31. Plot of Scores for Factor 2 for NIST Mirror Standard - 0.635  $\mu\text{m}$  to 0.935  $\mu\text{m}$

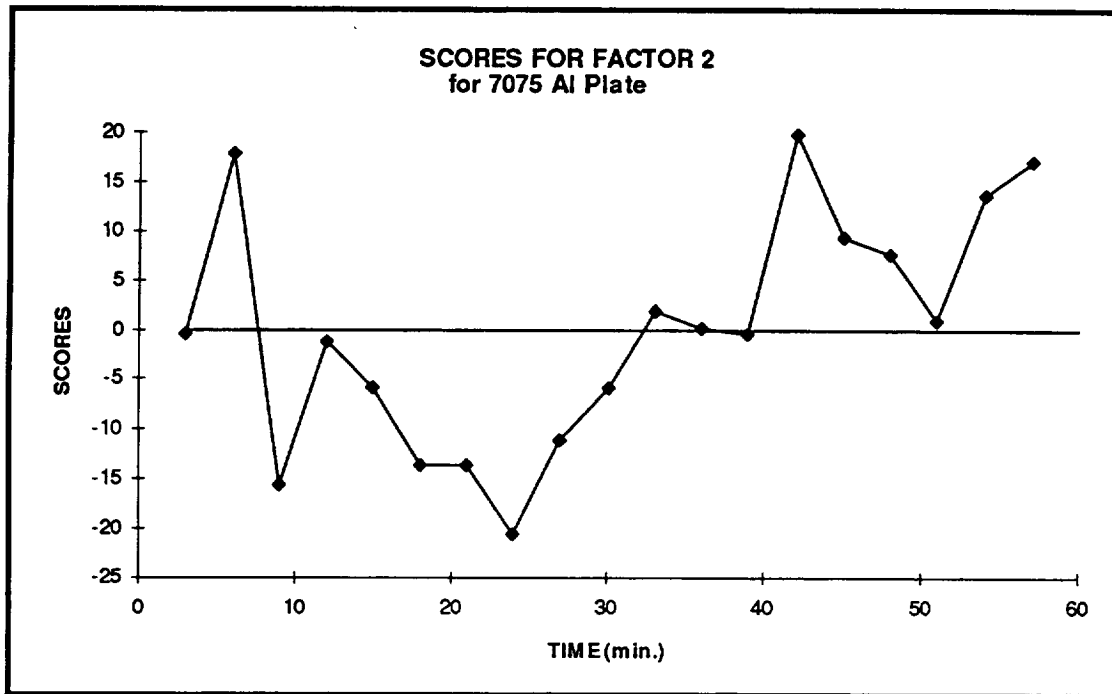
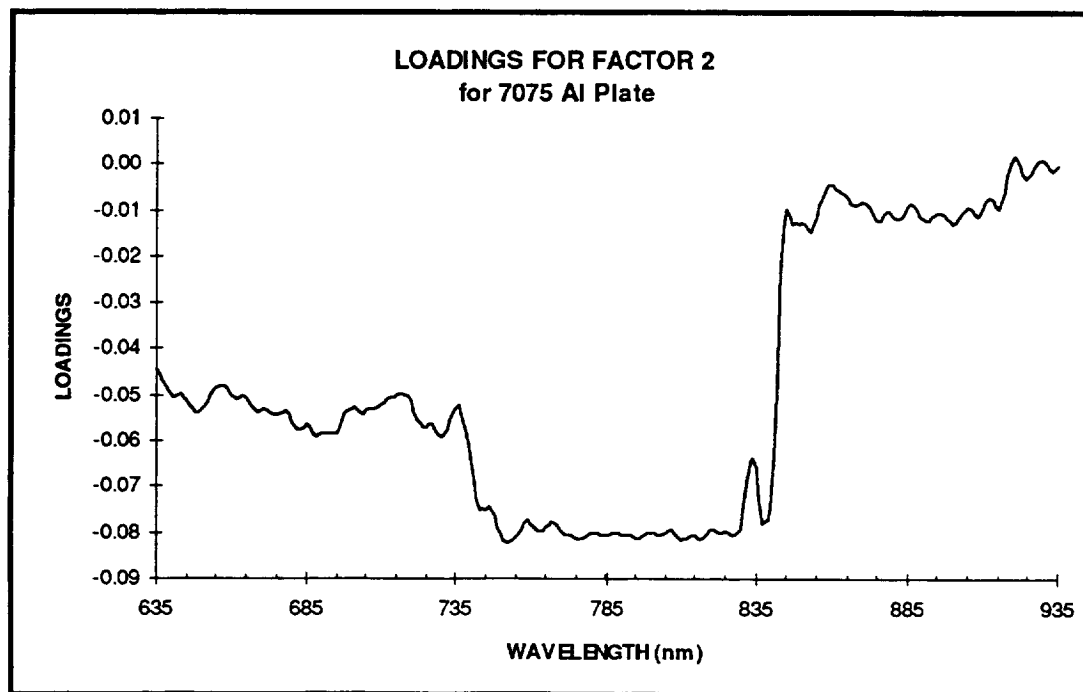


Figure 32. Plot of Loadings Factor 2 for NIST Mirror Standard - 0.635  $\mu\text{m}$  to 0.935  $\mu\text{m}$



Data was acquired with the Photo-Acoustics tri-beam ellipsometer to give a best fit for different  $n$  and  $k$  values for the substrate and the film. The initial assumption that the NBS Al mirror was not coated with any film was not able to obtain any sensible data. Next it was assumed that the aluminum substrate was coated with SiO, MgO, and MgF by substituting the appropriate values of  $n$  and  $k$  for the films. The only combination that gave sensible results was the SiO coating and it showed a film thickness of 3500Å. No indication of hydroxide or oxide film was obtained in these experiments. It is obvious that further work is required to bring the combined experimental capability of NIR and ellipsometry to bear with transient films as represented by the hydroxides of aluminum.

## 10.0 Conclusions

The results of these experiments have shown that NIR spectroscopy has the capability of quantitatively identifying many types of materials. The NIR fingerprint of mixtures can be very difficult to separate out; however, the use of multivariate analysis does provide some substantial improvement in both quantitation and identification of the influencing spectral features.

The experiments with the integrating sphere as a moderating influence on the surface spectral measurements were quite positive and merit continued work toward achieving a robotic system capable of scanning large structures such as the RSRM.

The combination of ellipsometry with NIR spectroscopy to monitor contaminants on surfaces did not work as well. The hardest part of the experiments was to correlate the presence of films on aluminum in humid conditions. There is too much variability in the films to obtain consistent data. The underlying factor may be that the ellipsometer is too sensitive for this particular measurement. More work is needed in this area to weed out the various options we should take to combine the capabilities of the two techniques.

## 11.0 Acknowledgements

We wish to express gratitude for the invaluable assistance of Ms. Yedilett Garlington in producing the many spectroscopic analyses of the experiments performed in this work and to Ms. Bianca Brindley and Mr. Garish Malapeddi for assisting in many of the other activities required to collect all the information compiled here. Thanks also go to Mr. Bill Nerren and Mr. Dewitt Burns at MSFC for their helpful suggestions and guidance in developing goals for this work.

## 12.0 References

1. K. Wefers and C. Misra, "Oxides and Hydroxides of Aluminum", Alcoa Technical Paper #19, Revised, 1987.
2. R. S. Alwitt, "The Aluminum-Water System", Oxides and Oxide Films 4 (1976) pp. 169-174, Dekkar.
3. J. B. Peri and R. B. Hannan, "Surface Hydroxyl Groups on  $\gamma$ -Alumina", J. Phys. Chem. 64 (1960) pp. 1526-1530.
5. J. B. Peri, "Infrared Gravimetric Study of the Surface Hydration of  $\gamma$ -Alumina", J. Phys. Chem. 69 (1965) pp. 211-219.
6. J.J. Fripiat, H. Bosemans, and P.G. Rouxhet, "Proton Mobility in Solids. I. Hydrogenic Vibration Modes and Proton Delocalization in Boehmite", J. Phys. Chem. 71 (1967) pp. 1067 - 1111.
7. R. K. Hart, "The Formation of Films on Aluminum Immersed in Water", Trans. Fara. Soc. 53 (1957) pp. 1020-1025.
8. Surface Treatment and Finishing of Aluminum and its Alloys, Vol. 1, S. Wernick, et.al. , ASM Internation, Metals Park, OH 1987

